Distributed Compressed Hyper spectral Image Sensing Using ADMM

Tomoya Hirakawa, Kazuki Chigita, and Yoshimitsu Kuroki
National Institute of Technology, Kurume College, Fukuoka, Japan
Email: {s53228th,kuroki}@kurume.kosen-ac.jp

***Abstract*—This paper describes a distributed compressed sensing method of HSI (Hyper Spectral Image). Similar to conventional methods, our method transfers computational load from encoder to decoder, and divides images into key and non-key frames. In video coding schemes, decoders interpolate non-key frames using motion vector or optical flow referring decoded key frames. However, the adjacent frames in wavelength domain have strong correlation at the same spacial positions. The PNSR of interpolated non-key frames would be high; then, our method applies ADMM (Alternating Direction Method of Multipliers) not only to reconstruct key and non-key frames but also to design the dictionaries of non-key frames. Experimental results show that the PSNR values of our method are about 3 to 5 dB higher than those of the method using DCT (Discrete Cosine Transform) for the dictionaries.**

***Keywords*—HSI, Distributed compressed image sensing, ADMM**

I. Introduction

General natural images consist of three spectral components: red green and blue. HSI (Hyper Spectral Image) has many spectral components including wavelengths outside the visible light, and specifies features of objects. Then HSI is applied for various fields: agriculture [3], medical imaging [4], and astronomy [5]. This paper discusses a distributed compressed sensing of HSI, which transfers computational cost from encoder to decoder. This feature of distributed compressed sensing contributes to the development of simple and low-energy-consumption cameras. The computational cost at the decoders is burdensome, but the structure of simple encoder and complex decoder has high affinity of an IoT (Internet of Things) society. Our method is based on a framework of distributed compressed video sensing [6], and similarly divides given frames, namely components of HSI, into key and non-key frames, and the original images are reconstructed by an optimize solver ADMM (Alternation Direction Method of Multipliers) [2,7] for convex error formulas. The key frames are decoded independently as intra frames, and the non-key frames are firstly interpolated by using already decoded key frames similar to inter-frames of movie sequences. The interpolated frames called side information are included to a formula to reconstruct the non-key frames. Since the adjacent pixels in spectral domain at the same spacial positions are highly correlated, the authors expect that generated side information would be very similar to the current non-key frame. Then, our method also designs non-key frames' dictionaries to represent given signals by using ADMM to improve reconstructed image quality.

II. Preliminaries

A. Compressed sensing

Compressed sensing is a problem of estimating sparse unknown vectors based on linear observations. If a given vector $\boldsymbol{f} \in \boldsymbol{R}^N$ is expressed by a linear combination of only K non-zero basis vectors by an orthonormal basis $\{\boldsymbol{v}_i\}$ $(i = 1, 2, \ldots, N)$, $\boldsymbol{f}$ is called K-sparse shown as

$$\boldsymbol{f} = \boldsymbol{\Upsilon}\boldsymbol{x} \quad s.t. \quad \|\boldsymbol{x}\|_0 = K, \tag{1}$$

where $\boldsymbol{\Upsilon} = (\boldsymbol{v}_1\boldsymbol{v}_2 \ldots \boldsymbol{v}_N)$, $\boldsymbol{x} \in \boldsymbol{R}^N$, and L_0 norm of $\boldsymbol{x}$, denoted as $\|\boldsymbol{x}\|_0$, is the number of non-zero elements of $\boldsymbol{x}$. For the K-sparse vector $\boldsymbol{x}$, one obtains a observation vector $\boldsymbol{y} \in \boldsymbol{R}^M (M < N)$. Here, the observation means an inner product $\boldsymbol{a}_i (i = 1, 2, \ldots, M)$ with $\boldsymbol{x}$. The observation process is expressed as

$$\boldsymbol{y} = \boldsymbol{A}\boldsymbol{f}, \tag{2}$$

where $\boldsymbol{A} \in \boldsymbol{R}^{M \times N}$ of which ith row is $\boldsymbol{a}_i$. For the number of elements and observations, Measurement Rate (MR) or the ratio of the number of row to column of the measurement matrix $\boldsymbol{A}$ is defined as follows:

$$MR = \frac{M}{N}. \tag{3}$$

Compressed sensing tries to reconstruct the original signal $\boldsymbol{f}$ only knowing the observation vector $\boldsymbol{y}$ and the observation matrix $\boldsymbol{A}$. Please note that the given vector $\boldsymbol{f}$ is K-sparse with respect to the basis matrix $\boldsymbol{\Upsilon}$; then, the reconstruction of $\boldsymbol{f}$ is formulated as

$$\min \|x\|_0 \quad s.t. \quad \boldsymbol{y} = \boldsymbol{A}\boldsymbol{f} = \boldsymbol{A}\boldsymbol{\Upsilon}\boldsymbol{x}. \tag{4}$$

However, since the L_0 norm minimization problem is NP-hard, it is often relaxed to the L_1 norm minimization problem as

$$\min \|x\|_1 \quad s.t. \quad \boldsymbol{y} = \boldsymbol{A}\boldsymbol{f} = \boldsymbol{A}\boldsymbol{\Upsilon}\boldsymbol{x}. \tag{5}$$

Its solution can be obtained efficiently since equation(5) is a linear programming problem.

978-1-5386-2615-3/18/$31.00 2018 IEEE

B. ADMM

ADMM is a convex optimization solver: ADMM obtains the optimal solution of convex functions on convex sets. If a function $g(\boldsymbol{x})$ follows the inequality

$$\frac{\alpha g(\boldsymbol{x}_1)+\beta g(\boldsymbol{x}_2)}{\alpha+\beta} \geq g\left(\frac{\alpha \boldsymbol{x}_1+\beta \boldsymbol{x}_2}{\alpha+\beta}\right) \tag{6}$$

for any two points $\boldsymbol{x}_1$ and $\boldsymbol{x}_2 \in \boldsymbol{R}^N$ and any real numbers α and β, this function g is convex. In a convex set $\boldsymbol{C}$, any $\boldsymbol{x}_1, \boldsymbol{x}_2 \in \boldsymbol{C}$ are closed to a convex combination $\frac{\alpha \boldsymbol{x}_1+\beta \boldsymbol{x}_2}{\alpha+\beta}$ for any real numbers α and β. ADMM can solve the constrained optimization problem expressed by the sum of two convex functions as

$$\min_{\boldsymbol{u},\boldsymbol{z}} \; g(\boldsymbol{u})+h(\boldsymbol{z}) \quad s.t. \boldsymbol{z}=\boldsymbol{G}\boldsymbol{u}. \tag{7}$$

Here, $\boldsymbol{G} \in \boldsymbol{R}^{N_2 \times N_1}$ is a full rank matrix, and g and h are convex functions of $\boldsymbol{u} \in \boldsymbol{R}^{N_1}$ and $\boldsymbol{z} \in \boldsymbol{R}^{N_2}$. ADMM finds the solution of equation (7) by the following iterations:

$$\boldsymbol{u}^{n+1}=\arg\min_{\boldsymbol{u}}\left\{g(\boldsymbol{u})+\frac{\rho}{2}\|\boldsymbol{z}^n-\boldsymbol{G}\boldsymbol{u}^n-\boldsymbol{d}^n\|_2^2\right\}, \tag{8}$$

$$\boldsymbol{z}^{n+1}=\arg\min_{\boldsymbol{u}}\left\{h(\boldsymbol{z})+\frac{\rho}{2}\|\boldsymbol{z}^n-\boldsymbol{G}\boldsymbol{u}^{n+1}-\boldsymbol{d}^n\|_2^2\right\}, \tag{9}$$

$$\boldsymbol{d}^{n+1}=\boldsymbol{d}^n+\boldsymbol{G}\boldsymbol{u}^{n+1}-\boldsymbol{z}^{n+1}, \tag{10}$$

where the superscript n means the nth iteration. Equation (9) can be rewritten as the proximal mapping or proximity operator

$$\boldsymbol{z}^{n+1}=prox_{\frac{1}{\rho}g}\left(\boldsymbol{G}\boldsymbol{u}^{n+1}+\boldsymbol{d}^n\right). \tag{11}$$

C. Distributed compressed video coding

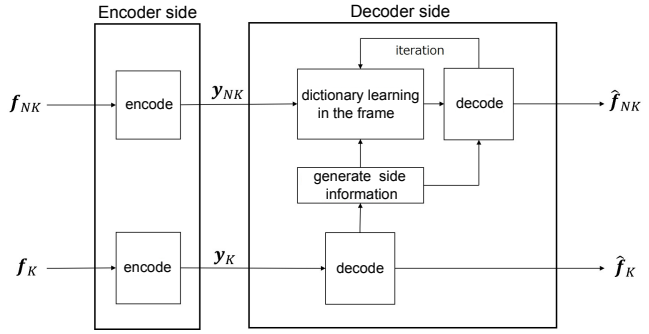

Fig. 1: Model of distributed compressed sensing using dictionary learning

The block diagram of distributed video sensing is illustrated in Fig.1, where input sequences are divided into key frames f_K's and non-key frames $\boldsymbol{f}_{NK}$'s. A key frame $\boldsymbol{f}_K$ is divided into non-overlapping blocks, and the ith block is represented as $\boldsymbol{f}_{K,i} \in \boldsymbol{R}^N (i=1,2,\ldots,B)$, where B is the number of blocks in the key frame. From here on we omit the index i since the encoding and the decoding processes are the same for all the blocks. A key frame $\boldsymbol{f}_K$ is decoded independently under the following optimization problem:

$$\hat{\boldsymbol{x}}=\arg\min_{\boldsymbol{x}}\left\{\frac{1}{2}\|\boldsymbol{y}_K-\boldsymbol{\Phi}_K\boldsymbol{\Psi}\boldsymbol{x}\|_2^2+\mu\|\boldsymbol{x}\|_1\right\} \tag{12}$$

Here, $\boldsymbol{\Psi}$ is the DCT matrix, $\boldsymbol{x}$ is the sparse coefficient of $\boldsymbol{\Psi}$, and μ is the weight of the regularization term. The encoding side transmits an observation vector $\boldsymbol{y}_K$ obtained by multiplying $\boldsymbol{f}_K$ by a low-rank random matrix $\boldsymbol{\Phi}_K$. The reconstructed frame $\hat{\boldsymbol{f}}_K$ is generated by calculating $\hat{\boldsymbol{f}}_K=\boldsymbol{\Psi}\hat{\boldsymbol{x}}$ using the solution $\hat{\boldsymbol{x}}$ of equation (12).

In the decoder of $\boldsymbol{f}_{NK}$, the side information $\boldsymbol{f}_{ave}$ is generated by reconstructed key frames. As expressed in previous sections, HSI has strong correlation in wavelength direction at the same spacial points; then, a $\boldsymbol{f}_{ave}$ is simply generated by averaging adjacent two key frames. The convex optimization problem for a non-key frame $\boldsymbol{f}_{NK}$ is formulated as

$$\begin{aligned}\min_{\boldsymbol{f}_{NK},\boldsymbol{x},\boldsymbol{D}} \; & \frac{1}{2}\|\boldsymbol{y}_{NK}-\boldsymbol{\Phi}_{NK}\boldsymbol{f}_{NK}\|_2^2 \\ & +\frac{\lambda_1}{2}\|\boldsymbol{f}_{NK}-\boldsymbol{D}\boldsymbol{x}\|_2^2+\mu\|\boldsymbol{x}\|_1+\lambda_2 h(\boldsymbol{f}_{NK}).\end{aligned} \tag{13}$$

Here, $\boldsymbol{y}_{NK}$ is a observation vector of non-key frame, and the original signal $\boldsymbol{f}_{NK}$ is assumed to be represented with a common dictionary of a target frame, denoted as $\boldsymbol{D}$, with sparse coefficient vector $\boldsymbol{x}$. The parameters λ_1, λ_2 and μ are weights of each term, $h(\boldsymbol{f}_{NK})$ is a regularization term

$$h(\boldsymbol{f}_{NK})=\|^t\boldsymbol{\Psi}(\boldsymbol{f}_{NK}-\boldsymbol{f}_{ave})\|_1, \tag{14}$$

which considers the differences of the original $\boldsymbol{f}_{NK}$ from the side information $\boldsymbol{f}_{ave}$: the differences are supposed to be sparse in the DCT domain.

III. PROPOSED METHOD

Sumi et al. proposed a scheme of compressed video coding of multi-view images [1], which employed ADMM to solve sparse expressions and furthermore to create dictionaries. We apply the same scheme for HSI whereas disparity compensation is not used for the side information as described below.

A. Key frame decoding

The convex optimization problem of $\boldsymbol{f}_K$ decoding is defined as (12); then, by setting $\boldsymbol{x}=\boldsymbol{a}=\boldsymbol{I}_N\boldsymbol{b}$, (12) is rewritten as

$$\min_{\boldsymbol{a},\boldsymbol{b}}\left\{\frac{1}{2}\|\boldsymbol{y}_K-\boldsymbol{\Phi}_K\boldsymbol{\Psi}\boldsymbol{a}\|_2^2+\mu\|\boldsymbol{b}\|_1\right\} \quad s.t. \quad \boldsymbol{b}=\boldsymbol{I}_N\boldsymbol{a}. \tag{15}$$

This problem can be solved with ADMM and the iterative formulas are gained by the simple deformation [1] as

$$\begin{aligned}\boldsymbol{a}^{n+1}=&\left\{^t(\boldsymbol{\Phi}_K\boldsymbol{\Psi})(\boldsymbol{\Phi}_K\boldsymbol{\Psi})+\rho\boldsymbol{I}_N\right\}^{-1} \\ &\left\{^t(\boldsymbol{\Phi}_K\boldsymbol{\Psi})\boldsymbol{y}_K+\rho(\boldsymbol{b}^n-\boldsymbol{c}^n)\right\},\end{aligned} \tag{16}$$

$$\boldsymbol{b}^{n+1}=Threshold(\boldsymbol{a}^{n+1}+\boldsymbol{c}^{n+1},\frac{1}{\rho}), \tag{17}$$

$$\boldsymbol{c}^{n+1}=\boldsymbol{c}^n+\boldsymbol{a}^{n+1}-\boldsymbol{b}^{n+1}, \tag{18}$$

where ρ is the weight parameter.

B. Non-key frame decoding

To solve equation (13) with ADMM, this study separates it into two optimization problems:

$$\min_{\boldsymbol{x},\boldsymbol{D}} \frac{\lambda_1}{2}\|\boldsymbol{f}_{NK} - \boldsymbol{D}\boldsymbol{x}\|_2^2 + \mu_1\|\boldsymbol{x}\|_1 + \mu_2\imath(\boldsymbol{D}), \quad (19)$$

$$\min_{\boldsymbol{f}_{NK}} \frac{1}{2}\|\boldsymbol{y}_{NK} - \boldsymbol{\Phi}_{NK}\boldsymbol{f}_{NK}\|_2^2 + \frac{\lambda_1}{2}\|\boldsymbol{f}_{NK} - \boldsymbol{D}\boldsymbol{x}\|_2^2 + \lambda_2\|{}^t\boldsymbol{\Psi}(\boldsymbol{f}_{NK} - \boldsymbol{f}_{ave})\|_1. \quad (20)$$

Here, μ_1 and μ_2 mean the weight of each term generated by division. The indicator function $\imath$ normalizes each column vector of $\boldsymbol{D}$. Equation (19) and (20) are a dictionary optimization and $\boldsymbol{f}_{NK}$ decoding problem respectively. Equation (19) includes the sparse coefficient $\boldsymbol{x}$ and the dictionary $\boldsymbol{D}$: this work solves equations (19) for $\boldsymbol{x}$ and $\boldsymbol{D}$ alternatively. Firstly, our method solves $\boldsymbol{x}$ for the temporarily fixed $\boldsymbol{D}$, and successively obtains $\boldsymbol{D}$ for $\boldsymbol{x}$ of the previous procedure. In both optimizations, the iterative formulas of ADMM are given by the deformations of quadratic form and proximally operation. Sumi et al. set $\boldsymbol{s} = \boldsymbol{r} = \boldsymbol{x}$ of (19), and show the solution $\boldsymbol{x}$ as

$$\boldsymbol{r}^{n+1} = (\lambda_1{}^t\boldsymbol{D}\boldsymbol{D} + \rho\boldsymbol{I}_N)^{-1} \left\{\lambda_1{}^t\boldsymbol{D}\boldsymbol{f}_{NK} + \rho(\boldsymbol{s}^n - \boldsymbol{r}^n - \boldsymbol{z}^n)\right\}, \quad (21)$$

$$\boldsymbol{s}^{n+1} = Threshold\left(\boldsymbol{r}^{n+1} + \boldsymbol{v}^n \cdot \frac{\lambda_1}{\rho}\right), \quad (22)$$

$$\boldsymbol{v}^{n+1} = \boldsymbol{v}^n + \boldsymbol{r}^{n+1} - \boldsymbol{s}^{n+1}. \quad (23)$$

Similarly, by setting $\boldsymbol{p} = \boldsymbol{q} = \boldsymbol{D}$, the solution $\boldsymbol{D}$ for the fixed $\boldsymbol{x}$ is given as follows:

$$\boldsymbol{p}^{n+1} = \left\{\lambda_1\boldsymbol{f}_{NK}{}^t\boldsymbol{x} + \rho(\boldsymbol{q}^n - \boldsymbol{w}^n)\right\} \left(\lambda_1\boldsymbol{x}^t\boldsymbol{x} + \rho\boldsymbol{I}_N\right), \quad (24)$$

$$\boldsymbol{q}^{n+1} = prox_{\rho\imath(\cdot)}\left(\boldsymbol{p}^n + \boldsymbol{w}^n\right), \quad (25)$$

$$\boldsymbol{w}^{n+1} = \boldsymbol{w}^n + \boldsymbol{p}^{n+1} - \boldsymbol{q}^{n+1}. \quad (26)$$

Next, we describe the solution $\boldsymbol{f}_{NK}$ of equation (20). The important point of (20) is the side information $\boldsymbol{f}_{ave}$. HSI captures the same still scene at various spectra, and there is no motion. Therefore, the proposed method does not offer motion compensation, and generate $\boldsymbol{f}_{ave}$ by the average of decoded adjacent two key frames. This is because correlation of adjacent frames is expected to be higher than that of moving images as shown in experiments. Equation (20) becomes as

$$\min_{\boldsymbol{f}_{NK}} \frac{1}{2}\|\boldsymbol{y}_{NK} - \boldsymbol{\Phi}_{NK}\boldsymbol{f}_{NK}\|_2^2 + \frac{\lambda_1}{2}\|\boldsymbol{f}_{NK} - \boldsymbol{D}\boldsymbol{x}\|_2^2 + \lambda_2\|\boldsymbol{l}\|_1 \quad s.t. \quad \boldsymbol{l} - {}^t\boldsymbol{\Psi}(\boldsymbol{f}_{NK} - \boldsymbol{f}_{ave}) = \boldsymbol{0}. \quad (27)$$

We apply ADMM for equation (27) and the iterative formulas are derived by the deformation of quadratic form, Cholesky decomposition and proximally operation [1] as follows:

$$\boldsymbol{f}_{NK}^{n+1} = ({}^t\boldsymbol{L})^{-1}\boldsymbol{L}^{-1}\left\{{}^t\boldsymbol{\Phi}_{NK}\boldsymbol{y}_{NK} + \lambda_1\boldsymbol{D}^{n+1}\boldsymbol{x}^{n+1} + \rho\boldsymbol{\Psi}(\boldsymbol{l}^n + {}^t\boldsymbol{\Psi}\boldsymbol{f}_{ave} + \boldsymbol{k}^n)\right\}, \quad (28)$$

$$\boldsymbol{l}^{n+1} = SoftThresh_{\frac{\lambda_2}{\rho}}\left({}^t\boldsymbol{\Psi}(\boldsymbol{f}_{NK} - \boldsymbol{f}_{ave}) - \boldsymbol{k}^n\right), \quad (29)$$

$$\boldsymbol{k}^{n+1} = \boldsymbol{k}^n + \boldsymbol{l}^{n+1} - {}^t\boldsymbol{\Psi}(\boldsymbol{f}_{NK}^{n+1} - \boldsymbol{f}_{ave}). \quad (30)$$

IV. Experiments

(a) Suwannee. (b) DC. (c) Cuprite.

Fig. 2: Images used in this experiments

We used three HSI sets for experiments. This study cuts and uses $256 \times 256 \times 32$ for each image. The first frames of each set are shown in Fig.2. Firstly, we illustrate the relation between the distance of frames in the spectral domain and the correlation is Fig.3. The figure indicates that the correlation does not vary drastically except for DC, and keeps high values even large frame distance. The block size of the key frames and

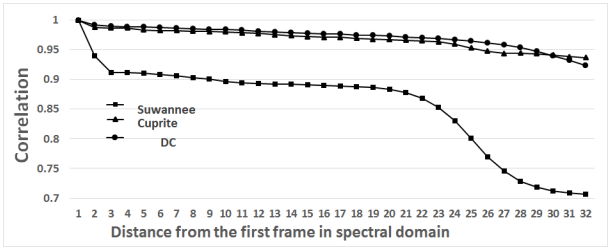

Fig. 3: The correlation values of each dataset

that of the non-key frames are 32×32 and 8×8 respectively. The reason why we use large blocks for key frame is that the key frames is similar to the intra frame, and HSI seems to have noise. Experiments show that MR for small blocks needs high value. Then, to decode key frames at reasonable observation ratio, we apply the block size as mentioned above. The observation matrices are random matrices with standard normal distribution. We assigned key frames every six frames in spectral domain to decrease the number of observations by increasing non-key frames, and all the five frames between adjacent key frames had the same side information. The weights are all set to one for simplicity. The observation ratio of $\boldsymbol{f}_K$ was 0.7 and that of $\boldsymbol{f}_{NK}$ was varied from 0.1 to 0.3. Decoded image quality is evaluated by PSNR.

Experiments were carried out for a method of using DCT without learning to compare our method. Table 1 shows PSNR values of the proposed method (P.M.) and the method using DCT for the dictionary of non-key frames. The results tell us that the proposed method improves PSNRs of Suwannee and Cuprite about 5dB, and the improvement of DC is decreased to 3dB. This would be caused because of many edges in the

DC image and rather low correlation shown in Fig.3. Figure 4 depicts actual decoded images, where the proposed method decreases block artifacts. Our method tries to optimize the sparse dictionary, which is compared with DCT in Fig.5. The designed dictionary contributes to the PSNR improvement.

TABLE I: PSNR average of reconstructed images[dB]

MR of key= 0.7						
	Suwannee		DC		Cuprite	
MR of non-key	DCT	P.M	DCT	P.M	DCT	P.M
0.10	19.572	25.913	17.950	21.547	20.054	26.298
0.15	19.992	26.185	18.280	21.846	20.451	26.504
0.20	20.730	26.494	18.877	22.138	21.196	27.148
0.25	20.700	26.699	18.933	22.397	21.152	27.382
0.30	21.816	27.127	19.777	22.712	22.246	27.729

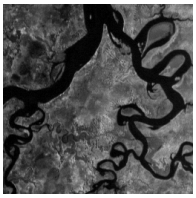
(a) Original


(b) DCT

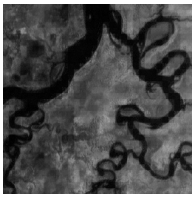
(c) Proposed method

Fig. 4: Original and reconstructed images by (b)DCT and (c)Proposed method

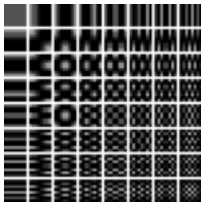
(a)DCT basis

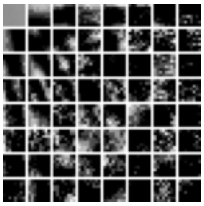
(b)A dictionary of proposed method

Fig. 5: Comparison of the two basis.

As shown in subsection *III*-B, our method divides (13) into sub-problems (19) and (20). Here, equation (19) employs a non-theoritical, heuristic, alternative solution to obtain $\boldsymbol{x}$ and $\boldsymbol{D}$. Figure 6 illustrates the convergence of the three solutions $\boldsymbol{x}$,$\boldsymbol{D}$ and $\boldsymbol{f}_{NK}$ for Suwannee. The vertical axis is the norm of differences between the temporal solutions at the current and at the previous iteration. Since all the graphs converge at around $n = 30$, whereas the norms of difference do not monotonically decrease. Then, figure 6 indicates that our solution is practical.

V. Conclusion

This paper has presented a distributed compressed sensing for hyper-spectral images. The encoder just calculate random projection for given images, and the decoder tries to reconstruct images based on convex formulas. This work has applies ADMM not only to reconstruct images but also to design the dictionaries for sparse representation. A part of our method is not theoretical but heuristic, but experimental results show

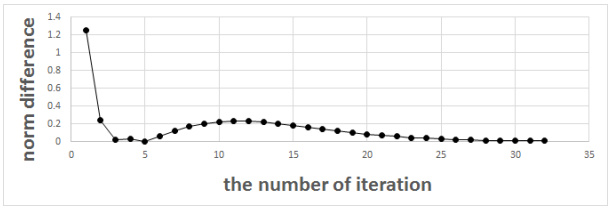

(a) $\boldsymbol{f}_{NK}$

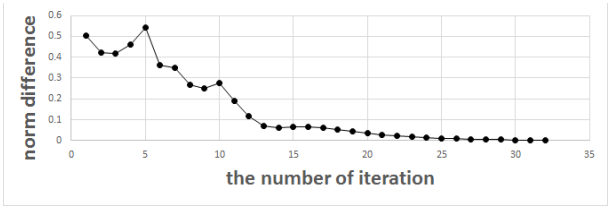

(b) $\boldsymbol{D}$

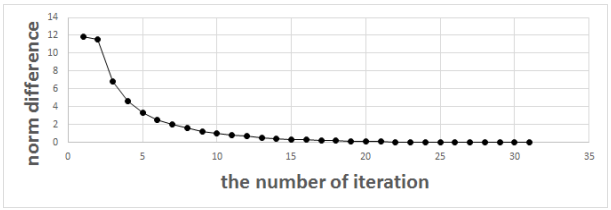

(c) $\boldsymbol{x}$

Fig. 6: Convergences of each variables of equation(13)

the superiority of our method in PSNR. Future works include theoretical analysis for solutions of multi-valuable formula.

Acknowledgement

This study is funded from the JSPS Grants-in-Aid for Scientific Research 15K00257.

References

[1] T. Sumi, I. Nakamura, and Y. Kuroki, "Distributed compressed video sensing of multi-view images using ADMM," Signal and Information Processing Association Annual Summit and Conference(APSIPA), 2016 Asia-Pacific, 2016.

[2] A. Rakotomamonjy, "Applying alternating direction method of multipliers for constrained dictionary learning," Neurocomputing. vol.106, pp.126-136, 2012.

[3] F.M. Lacer, M.M. Lewis, and I.T. Grierson, "Use of hyperspectral imagery for mapping grape varieties in the Barossa Valley, South Australia," IGARSS 2001. Scanning the Present and Resolving the Future. Proceedings IEEE 2001 International Geoscience and Remote Sensing Symposium, Sydney, pp.2875-2877, July 2001, doi:10.1109/IGARSS.2001.978191

[4] G. Lu and B. Fei, "Medical hyperspectral imaging: a review". Journal of Biomedical Optics, col.19 (1), pp.1-23, Jan. 2014, doi:10.1117/1.JBO.19.1.010901.

[5] E.K. Hege, D. O'Connell, W. Johnson, S. Basty, and E.L. Dereniak, "Hyperspectral imaging for astronomy and space surviellance". Proceedings of SPIE 5159, Imaging Spectrometry IX, pp. 380-391, Jan. 2004, doi:10.1117/12.506426.

[6] F. Tian, J. Guo, H. Liu, and H. Qin, "Distributed Compressed Video Sensing with Joint Optimization of Dictionary Learning and l_1-Analysis Based Reconstruction," IEICE Trans.Inf. Syst. volE99. no.4, pp. 1202-1211, 2016

[7] A. Rakotomamonjy, "Applying alternating direction method of multipliers for constrained dictionary learning," Neurocomputing. vol.106, pp.126-136, 2012